Flow and heat transfer of supercritical LNG in spiral microchannel

Yanyu Liu, *Tong* Su, *Xuan* Zhang, and *Yongou* Zhang[*]

School of Transportation, Wuhan University of Technology, Wuhan 430063, China.

Abstract. Liquefied natural gas (LNG) is stable and safe, which is why the natural gas is usually liquefied before transported. The heat exchanger is widely used as the key component of vaporizing LNG, and it is composed of a large number of microchannels. This paper mainly analyzes the flow of supercritical LNG in a spiral microchannel, and compares the flow and heat transfer characteristic of spiral microchannel with different pitch. The result was indicative that with the lessen of pitch, the heat transfer is improved, but the flow characteristic is decreased. Compared with the straight channel, the spiral channel with appropriate pitch value can markedly improve the heat transfer properties, but has less effect on the flow characteristic. The discussion also includes the flow and heat transfer of microchannel with different mass flux and heat flux.

Keywords: Heat exchanger; Spiral channel; Supercritical LNG.

1 Introduction

With the increasing global energy consumption, natural gas, due to its low carbon dioxide emission and high calorific value, has become the best choice to replace coal, oil and other traditional fossil energy [1]. The industrial chain related to liquefied natural gas (LNG) continues to develop, and the optimization of LNG storage, transportation, and utilization is of great significance. The heat exchanger is a key component in the vaporization process of LNG, and its optimization research is of high value.

In practical application, LNG needs to be pressurized above the critical pressure to reach the supercritical state, and then vaporized through the receiving station [2]. The interior of the heat exchanger is composed of many microchannels. It is found that the flow and heat transfer characteristics of fluid in the microchannel are obviously better than those in the conventional scale conditions, but the miniaturization of the scale will also cause large pressure drop and resistance [3]. Supercritical fluids have the advantages of high density, high heat conduction coefficient, low viscosity and fast diffusion speed [4]. The pressure drop and resistance generated by the flow in the micro-flow channel are greatly reduced, and better flow and heat transfer performance can be obtained [5]. The microchannel with the structure shape of staggered S-shaped fins can achieve a lower resistance pressure drop while ensuring good heat transfer performance. Literature have shown that curved flow channels of Z-type and S-type can ameliorate the heat transfer performance of heat exchanger, and better flow heat transfer performance can be obtained

---

[*] Corresponding author: zhangyo@whut.edu.cn

when the bending angle is 15° [6]. The microchannel with the structure shape of staggered S-shaped fins can achieve a lower resistance pressure drop while ensuring good heat transfer performance. Improving heat transfer performance and reducing pressure drop by changing the shape and structure of the runner is one of the main research directions for heat exchangers in recent years [7-13]. In this paper, the spiral microchannel is designed, and the flow and heat transfer performance of supercritical LNG in a single spiral microchannel with different shapes, different velocities or different heat flux are mainly simulated and discussed.

2 Microchannel for supercritical LNG flow

The basic microchannel model is a straight rectangular runner with a cross section of 2.0mm×1.85mm and a longitudinal length of 50mm. The rectangular section is divided into two domains: the inner supercritical LNG runner and the outer thermal conductive solid wall. The cross section of the inner domain is a semicircle with a radius of 0.75mm, as displayed in Fig. 1. In our present work, a spiral micro-flow channel is designed based on the straight microchannel model. The longitudinal distance advanced by a spiral rotation is the pitch p. The fluid domain models of basic straight channel, of p=50mm, p=25mm and p=16.67mm (p=50 mm, rotating 3 times) respectively are shown in Fig. 2.
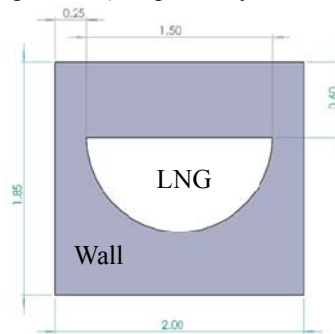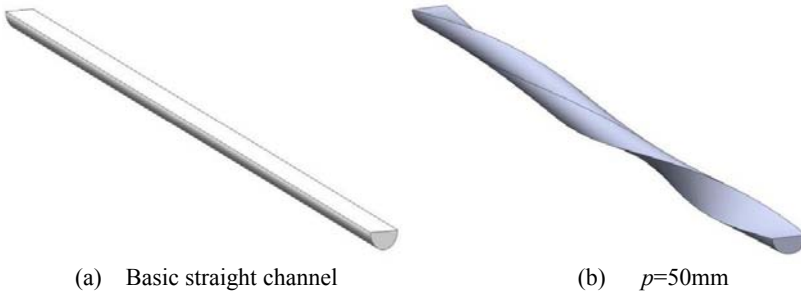

Fig. 1. Cross section of flow channel (Unit: mm).

(a)   Basic straight channel

(b) p=50mm

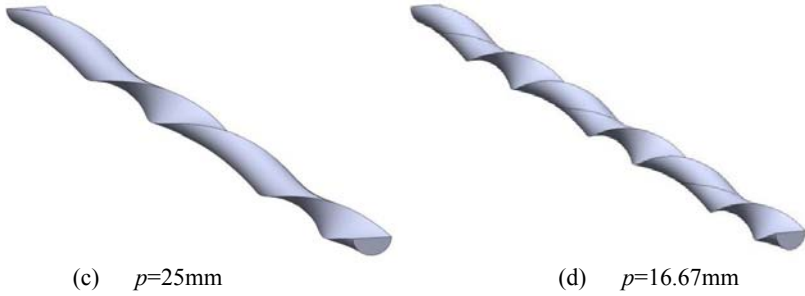(c) *p*=25mm   (d) *p*=16.67mm

Fig. 2. Microchannel with different shapes.

3 Simulate methods and validation

3.1 Turbulence model and boundary condition

The flow heat transfer of supercritical LNG in spiral microchannel is numerically simulated with steady-state calculation. The turbulence model is *K-ω* model, because of it can get better accuracy in internal flow, and the open energy equation. The boundary conditions are mass inlet and pressure outlet, and constant heat flux is applied on the upper and lower thermal conductive solid walls and its right and left walls are no slip wall.

3.2 Thermal physical properties

After fitting the thermophysical property curves used in reference [14], the parameter polynomials of thermophysical property are obtained as follows table1:

Table 1. The parameter polynomials of thermophysical property.

(1)ρ	
ρ=865.759-6.751T+0.0396786T^2-9.93909×10$^{-5}T^3$	(121≤T<233.65)
ρ=5606.645-53.738T+0.176T^2-1.94134×10$^{-4}T^3$	(233.65≤T<384.791)
(2)cp	
cp=-2940.78+129.48T-0.9449T^2+2.40359×10$^{-3}T^3$	(121≤T<162.12)
cp=-29299.31+585.69T-3.57T^2+7.39546×10$^{-3}T^3$	(162.12≤T<200.618)
cp=780505.89-11103.73T+52.66T^2-8.27359×10$^{-2}T^3$	(200.618≤T<218.679)
cp=15131340.31-269079.85T+1790.33T^2-5.28T^3+5.8255×10$^{-3}T^4$	(218.679≤T<236.74)
cp=-367428.36+4796.08T-20.25T^2+2.80547×10$^{-2}T^3$	(236.74≤T<260.504)
cp=169650.39-1620.37T+5.29T^2-5.78818×10$^{-3}T^3$	(260.504≤T<303.992)
cp=37704.89-285.23T+0.778489T^2-7.11777×10$^{-4}T^3$	(303.992≤T<361.74)
cp=3152.65	(361.74≤T<385)
(3)λ	
λ=0.34317-1.268×10^{-3}T-7.43911×10$^{-7}T^2$+4.035×10$^{-9}T^3$	(121≤T<233.413)
λ=2.333486-2.4318×10^{-2}T+8.63542×10$^{-5}T^2$-1.02523×10$^{-7}T^3$	(233.413≤T<284.268)
λ=0.350815-2.69×10^{-3}T+7.60346×10$^{-6}T^2$-6.82556×10$^{-9}T^3$	(284.268≤T<384.791)
(4)μ	
μ=1.283575×10^{-3}-2.1655×10^{-5}T+1.49×10$^{-7}T^2$-1.75047×10$^{-10}T^3$+5.77234×10$^{-13}T^4$	
	(121≤T<258.84)
μ=1.52655×10^{-5}	(258.84≤T<367.918)
μ=-5.813×10^{-5}+1.99×10^{-7}T	(367.918≤T<374.572)
μ=1.65929×10^{-5}	(374.572≤T<384.791)

where ρ, density; T, temperature, (K); cp, specific heat capacity; λ, thermal conductivity; μ, flow velocity.

According to table 1, the curves of cp and thermal conductivity change with temperature after polynomial fitting are displayed in Fig. 3.
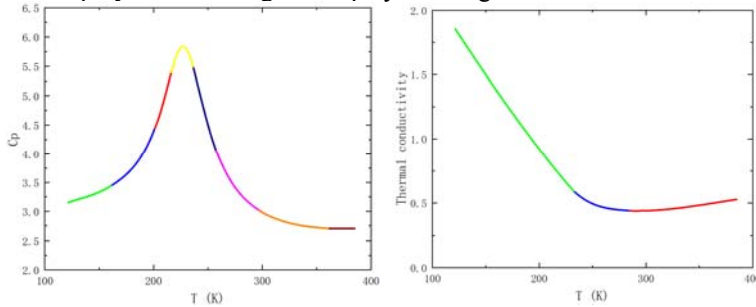

Fig. 3. Variation of c_p and thermal conductivity with temperature.

The intensity of convective heat transfer is expressed by Nusselt number:

$$Nu = \frac{hD_h}{\lambda} \tag{1}$$

where D_h, hydraulic diameter ; λ, thermal conductivity.

h is the convective heat transfer coefficient. It can be obtained by formula:

$$h = \frac{q_w}{T_{wall} - T_b} = \frac{q_w}{T_{wall} - (T_{out} + T_{in})/2} \tag{2}$$

where q_w, wall heat flux density, (W/m^2); T_{wall}, wall temperature; T_b, average of inlet temperature and outlet temperature; T_{in}, inlet temperature; T_{out}, outlet temperature.

The pressure loss expressed by Euler number is formulated as follows:

$$Eu = \frac{\Delta P}{\rho u^2} \tag{3}$$

where ΔP, pressure difference; ρ, denotes the density; and u, flow velocity.

3.3 Grid convergence

For the spiral model of p=25mm, three kinds of fluid computing grids are discussed respectively, including rough grid, normal grid and fine grid. The total numbers of grids corresponding to each grid scheme are 10 million, 20 million and 40 million units.

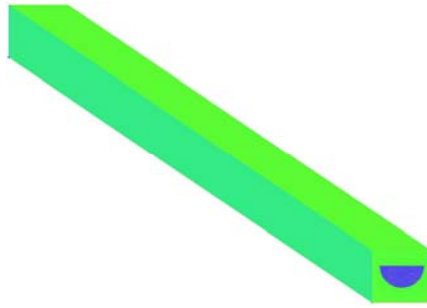The straight channel grid used in simulation is shown in Fig. 4.

Fig. 4. Mesh of 260mm straight channel.

In reference [14], when the mass flux of 260mm straight channel is 325kg/m^{2}s, the Eu number is 8.1401. The simulated Eu number is 8.2604, and the error is less than 2%.

The $y+$ values of three grids are mainly distributed between 0.1 and 1, and the grid at the entrance of different grids in Fig. 5.
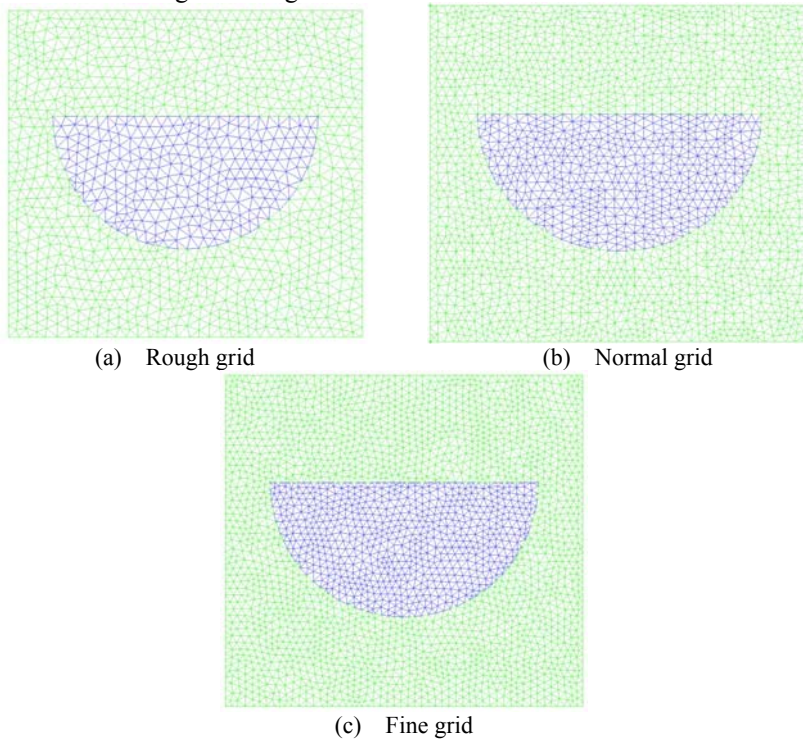

(a) Rough grid

(b) Normal grid

(c) Fine grid

Fig. 5. Inlet grid of different grid schemes.

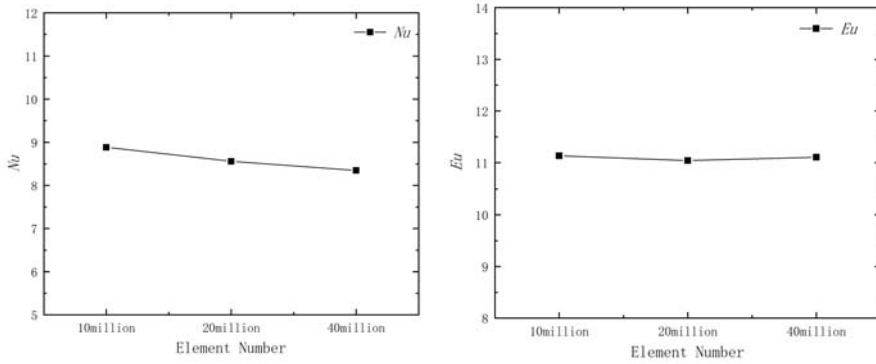Comparison of Nu and Eu numbers calculated under different grids are shown in Fig. 6.

Fig. 6. Comparison of *Nu* and *Eu* with different grid numbers.

In comparison of *Nu* with different grids numbers is shown that the heat transfer performance is very closely. As shown in comparison of *Eu* with different grids numbers, the pressure drop with the normal grid. So, the normal grid can meet the accuracy requirements.

4 Comparison of heat transfer flows in different shapes

CFD simulations are carried out for straight channel, of *p*=50mm, *p*=25mm and *p*=16.67mm microchannels with inlet mass flux of 325 kg/m^{2}s. The pressure of 10.5MPa and constant heat flow density of 30000 W/m^2 is applied to the upper and lower walls respectively.

A cross section is taken every 5mm. The temperature contours of different shapes in Fig. 7, and the velocity contours in Fig. 8. The upper right end of the figure is the inlet of the flow channel, the lower left end is the outlet of the flow channel, and the rest of the cross sections are arranged in sequence.
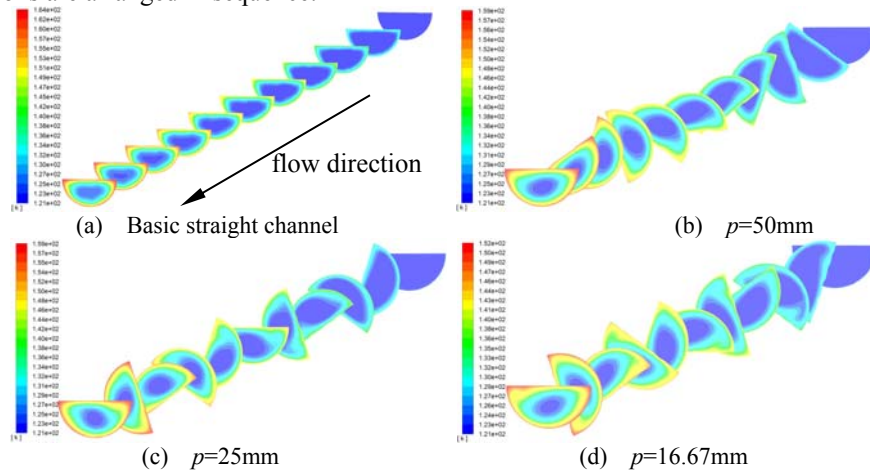

(a) Basic straight channel (b) *p*=50mm

(c) *p*=25mm (d) *p*=16.67mm

Fig. 7. Contours of temperature under different pitch.

(a)   Basic straight channel   (b)   *p*=50mm

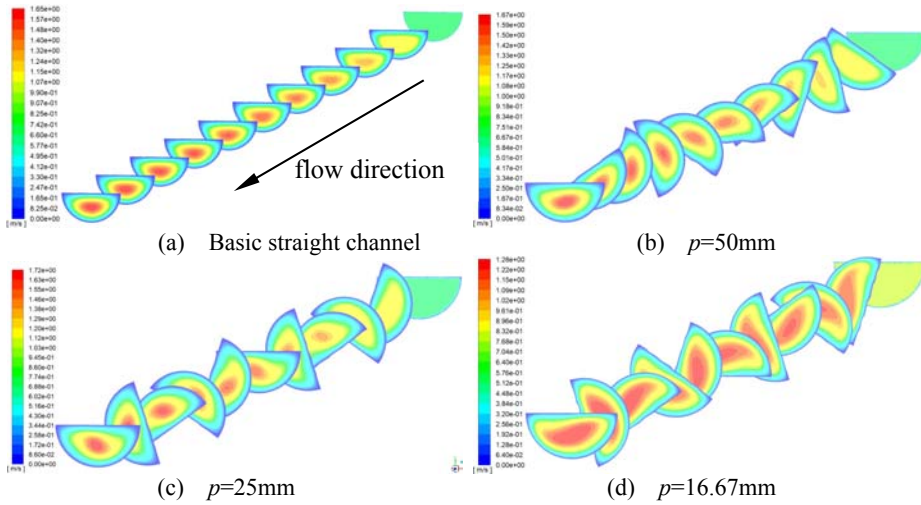(c)   *p*=25mm   (d)   *p*=16.67mm

Fig. 8. Contours of velocity under different pitch.

It can be seen from the contours that the temperature and speed of LNG increase with the flow direction. The LNG temperature in the center of flow channel is lower and the flow speed is faster. The flow in straight channel, the channel of *p*=50mm and of *p*=25mm are more stable, while the flow in channel of *p*=16.67mm is worse.

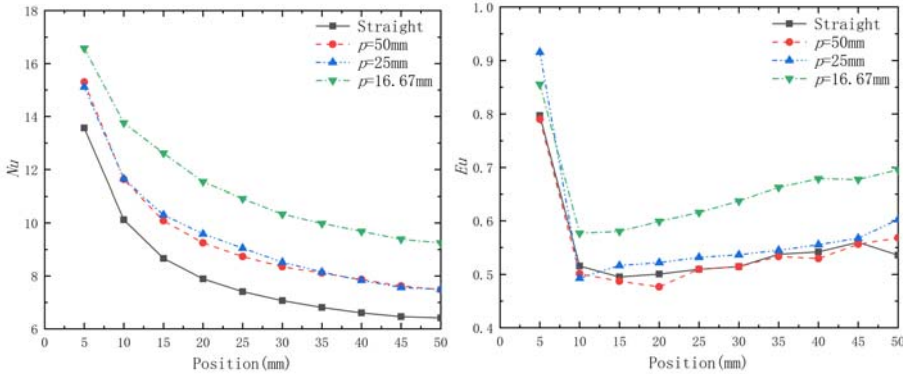Comparison of *Nu* and *Eu* numbers are shown in Fig. 9.

Fig. 9. Comparison of local *Nu* and *Eu* numbers in different geometric shapes.

According to the Fig. 9, with the grow in rotation angle, the heat transfer effect will also be enhanced. Among them, the heat transfer effect of the microchannel with pitch of 16.67mm is significantly better than other shapes, because of it have the higher *Nu,* while the pressure loss of the channel with pitch of 16.67mm is the worst with the higher *Eu*. In addition, the heat transfer effect of the microchannel with pitch of 50mm and 25mm are also significantly better than that of the straight channel. And that the pressure loss of straight channel, the channel with pitch of 50mm and of 25mm have little difference.

5 Comparison of heat transfer flows at different velocities

CFD simulation is carried out for the microchannel *p*=25mm under the conditions of inlet mass fluxes of 200kg/m^{2}s, 325kg/m^{2}s, 450kg/m^{2}s, 575kg/m^{2}s, 700kg/m^{2}s, pressure of 10.5MPa, and constant heat flux of 30000W/m^2 on the upper and lower walls. The

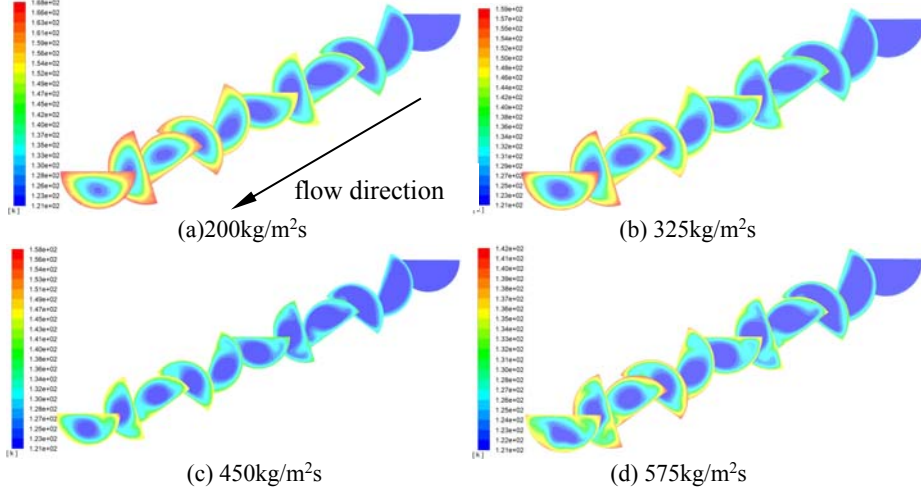temperature contours at different flow rates, as illustrated in Fig.10, and the velocity contours in Fig.11.

(a)200kg/m^{2}s   (b) 325kg/m^{2}s

(c) 450kg/m^{2}s   (d) 575kg/m^{2}s

Fig. 10. Contours of temperature under different mass fluxes.

(a) 200kg/m^{2}s   (b) 325kg/m^{2}s
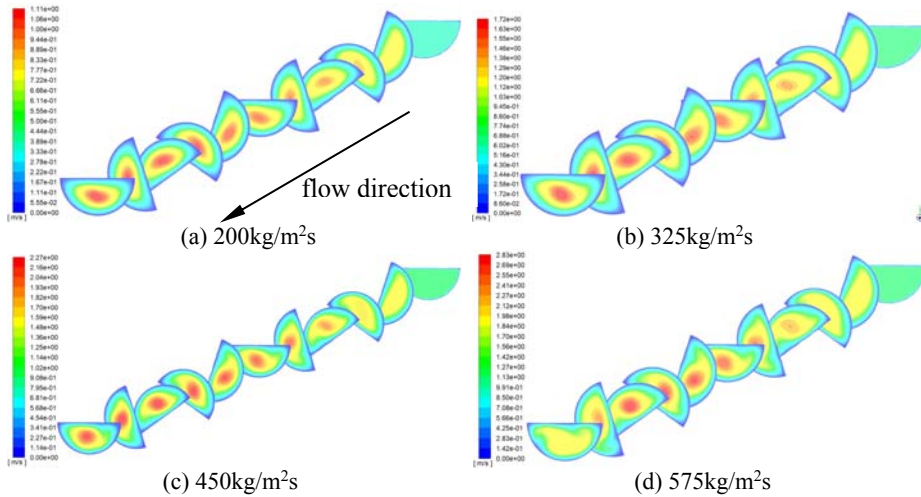
(c) 450kg/m^{2}s   (d) 575kg/m^{2}s

Fig. 11. Contours of velocity under different mass fluxes.

It can be making out from Fig.10 and Fig.11, the flow is relatively stable when the mass flux is 200kg/m^{2}s and 325kg/m^{2}s, while the flow becomes chaotic when the mass flux exceeds 450kg/m^{2}s.

Comparison of *Nu* and *Eu* under different mass fluxes are displayed in Fig. 12.
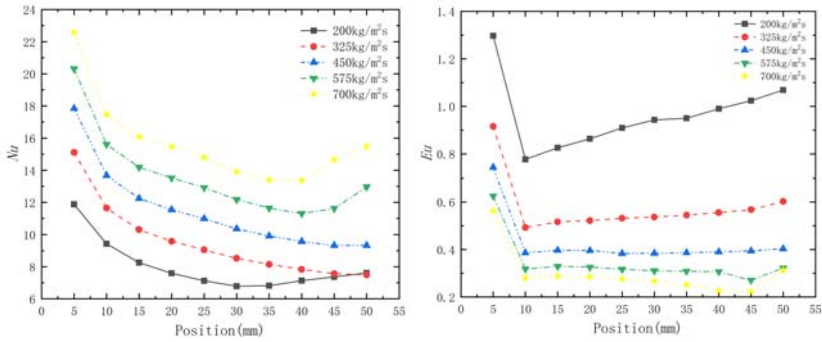
Fig. 12. Comparison of local *Nu* and *Eu* numbers at different mass fluxes.

In Fig. 12, with the increase of mass flux, *Nu* number increases while *Eu* number decreases, and both heat transfer and flow characteristic are improved. However, when mass flux exceeds 450kg/m^{2}s, flow characteristic has little room for improvement.

6 Comparison of heat transfer flow conditions under different heat flux

In the case of different heat flux on the above and below the thermal conductive solid wall. The temperature contours under different heat flux have similar variation tendency along the flow direction (Fig. 13). As displayed in Fig. 14, the flow in different heat flux is stable.
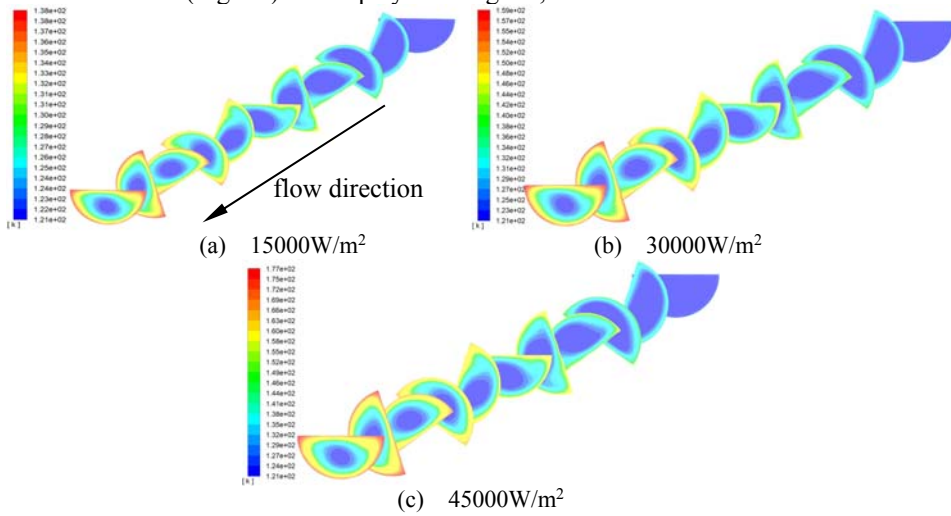

(a)   15000W/m^2

(b)   30000W/m^2

(c)   45000W/m^2

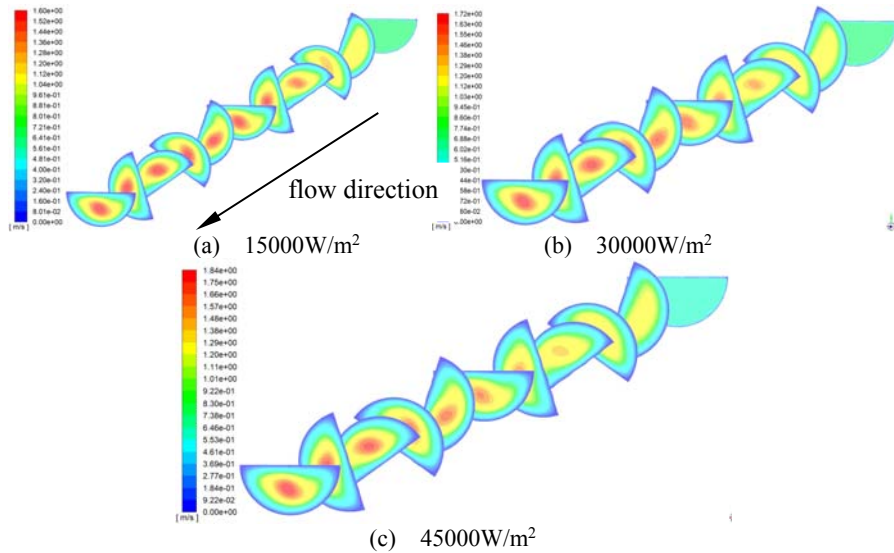**Fig. 13.** Contours of temperature under different heat flux.

Fig. 14. Contours of velocity under different heat flux.

CFD simulation is carried out on the microchannel with 25mm pitch under the condition that mass flux at the inlet was 325kg/m²s. The pressure is 10.5MPa, and heat flux of 15000W/m², 30000W/m², and 45000W/m² are applied on the above and below the thermal conductive solid wall respectively. The comparison figure of *Nu* and *Eu* was obtained, as displayed in Fig. 15.
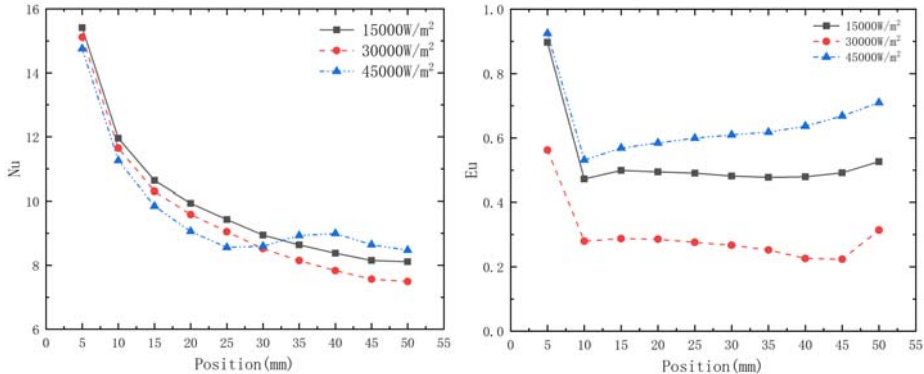

Fig. 15. Comparison of local *Nu* and *Eu* under different heat flux.

In Fig.15, under different heat flux the heat transfer characteristic there are similar values in the same position. And that in the comparison of local *Eu* under different heat flux, the heat flux with 30000W/m² have the *Eu* number, it means that the flow characteristic is the best when the heat flux is 30000W/m².

7 Conclusion

The flow and heat transfer of supercritical LNG flowing in a single spiral microchannel is simulated. According to the section 4, the channel with more turns shows better heat transfer characteristic. In the light of both flow and heat transfer performance, when the channel radius is 0.75mm, the channel with the pitch of 50mm obtain better heat transfer than straight channel, and has inapparent effect on the flow characteristic.

In the spiral microchannel, the heat transfer performance is improved with the acceleration of flow velocity. With the increase of the heat flux of the upper and lower thermal conductive solid walls, the heat transfer performance changes little, and the flow characteristic in the heat flux of 30000W/m^2 have the lowest *Eu* number.

Acknowledgements

References

1. A. Yousefi, M. Birouk, Investigation of natural gas energy fraction and injection timing on the performance and emissions of a dual-fuel engine with pre-combustion chamber under low engine load[J]. Applied Energy, Volume **189**,2017, 492-505,0306-2619,

2. S.S. Liu, W.L. Jiao, P. Zhang, Conjugate numerical analysis on bundle effects for integrated heat transfer of LNG ambient air vaporizer[J]. Applied Thermal Engineering,2020,**180**.

3. D.C. Denkenberger, M. J. Brandemuehl, J. Zhai, J.M. Pearce, Finite Difference Heat Exchanger Model: Flow Maldistribution with Thermal Coupling[J]. Heat Transfer Engineering,2021,**42**(11).

4. Y.Y. Bae, A new formulation of variable turbulent Prandtl number for heat transfer to supercritical fluids. International Journal of Heat and Mass Transfer. Volume **92**,2016,792-806, 0017-9310.

5. W. Qu, I. Mudawar, Experimental and numerical study of pressure drop and heat transfer in asingle-phase micro-channel heat sink. Intemational Journal of Heat and Mass Transfer, 2002, **45**, 2549-2565.

6. D.D. Jia, Z.C. Zhao, Y. Zhang, Y.M. Zhou, Y.R. Zhang, L. Zhang, Numerical Study of Flow and Heat Transfer Characteristics of Supercritical LNG in Micro-channel of Printed Circuit Vaporizer[J]. Ship Engineering, 2017,**39**(05):35-40.(In Chinese)

7. D.O. Ariyo, T. Bello-Ochende, Constructal design of two-phase stacked microchannel heat exchangers for cooling at high heat flux[J]. International Communications in Heat and Mass Transfer,2021,**125**.

8. F. Zhou, W. Zhou, C.Y. Zhang, Q.F. Qiu, D. Yuan, X.Y. Chu, Experimental and numerical studies on heat transfer enhancement of microchannel heat exchanger embedded with different shape micropillars[J]. Applied Thermal Engineering,2020,**175**.

9. Z.Y. Guo, Z.X. Li. Size effect on single-phase channel flow and heat transfer at microscale. International Journal of Heat and Fluid Flow, 2003, **24**(3), 284-298.

10. P. Gao, S. L. Peterson, M. Favre-Marinet, Scale effects on hydrodynamics and heat transfer intwo-dimensional mini and microchannels. International Journal of Thermal Science, 2002, **41**, 1017-1027.

11. C.X. Lin, M. A. Ebadian, The effects of inlet turbulence on the development of fluid flow and heat transfer in a helically coiled pipe[J]. International Journal of Heat & Mass Transfer, 1999, **42**(4):739-751.

12. L. J. Li, C. X. Lin, M. A. Ebadian, Turbulent heat transfer to near-critical water in a heated curved pipe under the conditions of mixed convection[J]. International Journal of Heat & Mass Transfer, 1999, **42**(16):3147-3158.

13. M. B. Sharabi, W. Ambrosini, S. He, Prediction of unstable behaviour in a heated channel with water at supercritical pressure by CFD models[J]. Annals of Nuclear Energy, 2008, **35**(5):767-782.

14. Z.C Zhao, K. Zhao, D.D. Jia, P.P. Jiang, R.D. Shen, Numerical Investigation on the Flow and Heat Transfer Characteristics of Supercritical Liquefied Natural Gas in an Airfoil Fin Printed Circuit Heat Exchanger[J]. Energies,2017,**10**(11).